Ann. For. Res. 66(1): 63-77, 2023
https://doi.org/10.15287/afr.2023.2548

ANNALS OF FOREST RESEARCH
www.afrjournal.org

Detection of invasive plants using NAIP imagery and airborne LiDAR in coastal Alabama and Mississippi, USA

Nisham Thapa[1]✉, Lana L. Narine[1], Zhaofei Fan[1], Kasip Tiwari[1]

Thapa N., Narine L.L., Fan Z., Tiwari K., 2023. Detection of invasive plants using NAIP imagery and airborne LiDAR in coastal Alabama and Mississippi, USA. Ann. For. Res. 66(1): 63-77.

Abstract: Invasive plants have imposed severe threats to native ecosystems worldwide. *Triadica sebifera* (Tallow tree) and *Ligustrum sinense* (Chinese privet) are among the most prolific invasive species in the southern United States (US) that needs urgent assessment to protect coastal ecosystems. The lack of spatially explicit assessments of these invasives, coupled with the increasing availability of high-resolution remotely sensed data, represents an opportunity to produce a distribution map for subsequent monitoring. The overall goal of this study was to develop spatially comprehensive maps of Tallow tree and Chinese privet in ecologically sensitive coastal regions, where both invasives have become well established. The study was conducted in three coastal sites within Alabama and Mississippi: (1) Mobile Tensaw River Delta, (2) Bon Secour National Wildlife Refuge, and (3) Mississippi Sandhill Crane National Wildlife Refuge. We implemented three image classification methods, representing unsupervised, supervised, and machine learning techniques, respectively: (1) ISODATA, (2) Maximum Likelihood (ML), and (3) Random Forest (RF). For each classification, a 1 m National Agriculture Imagery Program (NAIP) orthoimage was first examined, then integrated with vegetation structure and topography parameter derived from airborne light detection and ranging (LiDAR). The maximum Overall Accuracy (OA) of 87.5% was obtained using RF model with NAIP stacked image integrated with LiDAR derived variables. Overall, findings highlight the potential for accurately characterizing both Tallow tree and Chinese privet using readily available remote sensing data. Mapped products from this study represent a spatially comprehensive baseline inventory of crucial invasive species and will serve to inform the development of a framework for broader-scale mapping and monitoring efforts.

Keywords: invasive, LiDAR, classifier, random forest.

Addresses: [1]College of Forestry, Wildlife and Environment, Auburn University, Auburn, Alabama, USA.

✉**Corresponding Author:** Nisham Thapa (nzt0037@auburn.edu)

Manuscript received August 11, 2022; revised June 2, 2023; accepted July 3, 2023.

Introduction

Invasive plants are defined as species whose introduction causes or is likely to cause economic or environmental harm, or harm to human health (Order Executive 1999). They impair soil nutrient cycling and alter forest stand structure (Ehrenfeld 2010). The infestation of invasive plants has significantly threatened native plants listed under the Endangered Species Act in almost half of the

US ecosystems (Wilcove et al. 1998). For instance, invasive plants have caused a decline of 42% of the US endangered and threatened species (Order Executive 1999). In addition, the control cost of invasion has increased from $2 billion in 1960-1969 to $21 billion in 2010-2020 (Fantle-Lepczyk et al. 2022).

Several invasive species are well-established across the southeastern US. For instance, among the ten most prominent invasive plants in Alabama according to the Alabama Invasive Plant Council are, Tallow tree and Chinese privet (ALIPC 2019). Both invasive plants are native to China and were introduced to the US in 1852 for ornamental purposes (Hanula & Horn 2009, Wang 2011). Tallow tree is a deciduous tree that can grow up to 18.3 m high and 0.9 m wide at maturity. The main pathways for seed dispersion are birds and disturbances, such as hurricanes and floodwater (Yang et al. 2021). Tallow tree contains high tannins in the leaf litter, that alters the composition of microbial communities and eventually displaces native species (Montez et al. 2021). In the south-eastern US, from North Carolina south to Florida and west through Louisiana and Arkansas to Texas, Tallow tree has invaded wet coastal areas and spread rapidly inland. Around $518 million of timber loss is estimated within the next 20 years if no effective control measures for Tallow tree is applied (Wang 2011). Chinese privet is a semi-evergreen to evergreen shrub that can grow up to 10 m. It propagates by root sprouts, and seed dispersal is carried out mainly by birds and other wildlife. It has a negative impact on native plant abundance and diversity (Wilcox & Beck 2007, Foard 2014), limits forest regeneration (Loewenstein & Loewenstein 2005, Cash et al. 2020), and produces a monoculture (Hart & Holmes 2013). Furthermore, it has been implicated in the decline of species of conservation concern, such as the *Sarracenia oreophila* (green pitcher plant) and *Helianthus schweinitzii* (Schweinitz's sunflower) (Cash et al. 2020). Estimated control cost of Chinese privet ranges from $216–$1,820 per ha (Klepac et al. 2007, Benez-Secanho et al. 2018). Around $2.72 billion of timber loss, within the next 20 years, is estimated if no effective control measures for Chinese privet is applied (Wang 2011).

Field surveys can be used to collect detailed information on invasive plant species; however, studies (Zuberi et al. 2014, Ismail et al. 2016) have noted that this approach is not sustainable for large geographical areas due to labor, time, capital constraints, and difficulty in accessing remote areas of interest. On the other hand, remote sensing technologies have been increasingly used for invasive plants mapping due to the capability to provide synoptic views over large geographical and inaccessible areas (Huang & Asner 2009, Matongera et al. 2018). Several studies have shown that using remotely sensed data to map invasive plants may be a viable option. For example, Bradley (2014) explored spectral, textural, and phenological approaches for remote detection of invasive plants. Another study, Ismail et al. (2016) found that the synergy of multi-source remotely sensed data could increase image classification accuracy.

Many studies highlight higher accuracy in detection and vegetation mapping using LiDAR combined with high-resolution multispectral imagery (Asner et al. 2008, Kim et al. 2020, Liang et al. 2020). LiDAR uses laser light to derive three-dimensional information (Popescu 2007). Asner et al. (2008) explained that LiDAR, when combined with imagery could be used to detect woody invasive tree species, such as *Fraxinus uhdei*, *Myrica faya*, and *Psidium cattleianum*, for studying the presence and abundance of species. The use of aerial imagery and LiDAR-derived products increases the potential for detecting invasive species, particularly for taller, woody invasives (Dubayah & Drake 2000, Asner et al. 2008, Hantson et al. 2012). For instance, Hantson et al. (2012) demonstrated that LiDAR-derived products using ML classification increased the classification accuracy from 39% to 50% for woody invasive species. The use of aerial

imagery alone underestimated the classification of shrub vegetation, but the integration of LiDAR and imagery helps distinguish shrub vegetation from tall trees (Bork & Su 2007).

Image classification techniques like Iterative Self Organizing Data Analysis Technique (ISODATA) and ML classifier are used as traditional techniques to map invasive plants (Ustin et al. 2002, Michez et al. 2016, Mohler & Morse 2022). Over the last two decades, machine learning algorithms have been widely used to classify invasive plants and demonstrate the ability to obtain accurate and reliable information from satellite imagery (Calvino-Cancela et al. 2014, Singh et al. 2015, Jensen et al. 2020). Among machine learning methods described in the literature, RF is considered desirable for multi-source classification of remote sensing data (Gislason et al. 2006). Several studies have demonstrated its superiority for high-dimensional input data such as hyperspectral and multi-source data , even with limited training data (Ham et al. 2005, Chan et al. 2012, Abdel-Rahman et al. 2014, Jensen et al. 2020, Shoot et al. 2021). Kim et al. (2020) conducted vegetation mapping with LiDAR and multispectral imagery using four different classification algorithms (Support Vector Machine (SVM), RF, ML, and Mahalanobis Distance). RF classification using NAIP-LiDAR stacked image provided the highest OA (75.7%). Another study, Liang et al. (2020) carried out vegetation mapping by using three classification approaches (Object-based image analysis, RF, and SVM on high-resolution multispectral imagery. LiDAR data used with RF gave the highest user's accuracy (96%) for classifying *Pueraria montana* (Kudzu).

A study on Tallow tree mapping across a 48.25 km^2 coastal region of Texas-Louisiana showed classification accuracies greater than 95% at 0.5 m and 1 m spatial resolution using color-infrared photography (Ramsey et al. 2002). Authors used imagery collected during senescence when leaves of Tallow tree were bright red, but observed that not all senescing tallow leaves were bright red. Another study conducted on the coastal region of the southern U.S. observed an overall classification accuracy of 80% for mapping Tallow tree using RF (Randall 2015). The application of remote sensing data for mapping Chinese privet is limited. A study using citizen science data showed 84% accuracy in mapping Chinese privet over a study area of 0.72 km^2 in Georgia (Hawthorne et al. 2015). In Cash et al. (2020), moderate resolution multispectral images (Landsat 8 and Sentinel 2) were used to map Chinese privet at a 30 m and 10 m spatial resolution over a 23 km^2 study site and obtained an overall accuracy of 92.3% using the ML. This work highlights the utility of satellite imagery for detecting dense monocultures of Chinese privet with high accuracy.

Although previous studies have focused on mapping Tallow tree (Ramsey et al. 2002, Randall 2015) and Chinese privet (Hawthorne et al. 2015, Barnett 2016, Cash et al. 2020b) over a small spatial extent, the potential of freely available remotely sensed data for mapping invasive plants over larger areas has not been investigated. There is especially a need to develop effective methods for detecting and mapping understory invasive species (Joshi et al. 2004). More importantly, to date, there are no spatially explicit fine-scale maps of Tallow tree and Chinese privet for coastal Alabama and Mississippi. Such maps can support decision-making for effective invasive species management and to moderate their spread in the coastal area. Coastal ecosystems are ecologically important and sensitive to global climate (Heckbert et al. 2011, Ng et al. 2021). They are especially vulnerable to invasive plants as they can form monotypic stands and impact nutrient cycling (Zedler & Kercher 2004, Bush et al. 2020). The study of invasive species in the coastal areas can help researchers understand the associated factors that facilitate the growth and spread of invasives. The increasing availability of airborne LiDAR and NAIP imagery presents an exceptional convenience to achieve detailed, finer-scale observations for invasive species

assessments.

This study's overall goal was to develop approaches for detection and distribution mapping of Tallow tree and Chinese privet in the coastal region of Alabama and Mississippi using available remotely sensed data. With a focus on three study sites, this work specifically served to:

a. Develop a methodology for detecting Tallow tree and Chinese privet using airborne LiDAR and NAIP imagery, and

b. Characterize the spatial extent and coverage of Tallow tree and Chinese privet.

Materials and Methods

To meet the study's overall goal, NAIP imagery and airborne LiDAR data from United States Geological Survey's 3D Elevation Program (USGS 3DEP) (U.S. Geological Survey 2020a) were examined and field verification was conducted. Bands of NAIP imagery and a NAIP derived vegetation index, Normalized Difference Vegetation Index (NDVI) were integrated with LiDAR-derived variables, such as Canopy Height Model (CHM) and Topographic Wetness Index (TWI) for the image classification. Three classification methods (unsupervised, supervised and machine learning technique) were applied using various combinations of spectral bands, vegetation index and airborne LiDAR-derived parameters to determine potential improvement in invasives' detection. The overall workflow of the study is shown in Figure 1.

Study area

The study was carried out within Mobile Tensaw River Delta (Mobile Tensaw), Bon Secour National Wildlife Refuge (Bon Secour), and Mississippi Sandhill Crane National Wildlife Refuge (Mississippi Sandhill) located in the coastal region of southern Alabama and Mississippi (Figure 2). The study region is classified as a humid subtropical climate with an average annual temperature of 18°C (64°F). The temperature in the hottest month (July) and coldest month (January) averages 32°C (90°F) and 4°C (40°F), respectively. The region's average annual precipitation is 1,400 mm. The landform consists of flat plains, marshes, bogs, swamps, and river deltas and is mostly dominated by prairie ecosystem, wetlands, submerged grass beds, pine flatwoods, wet pine savanna ecosystem, and bottomland hardwoods. The area for the study extents of Mobile Tensaw, Bon Secour, and Mississippi Sandhill were 751 km², 20.03 km² and 4.74 km², respectively. Mobile Tensaw is one of the largest wetland ecosystems of the US and is a biologically diverse region that offers home to endangered freshwater mussels (Handley et al. 2013). Bon Secour protects the coastal barrier of Alabama and provides habitat to threatened species, such as Alabama beach mouse and green, loggerhead, and Kemp's ridley turtle (U.S. Fish and Wildlife Service 2023a). Mississippi Sandhill restores the last remaining wet pine savanna ecosystem, a pivotal habitat for critically endangered Mississippi Sandhill cranes, songbirds, waterfowls, and dusky gopher frog (U.S. Fish and Wildlife Service 2023b).

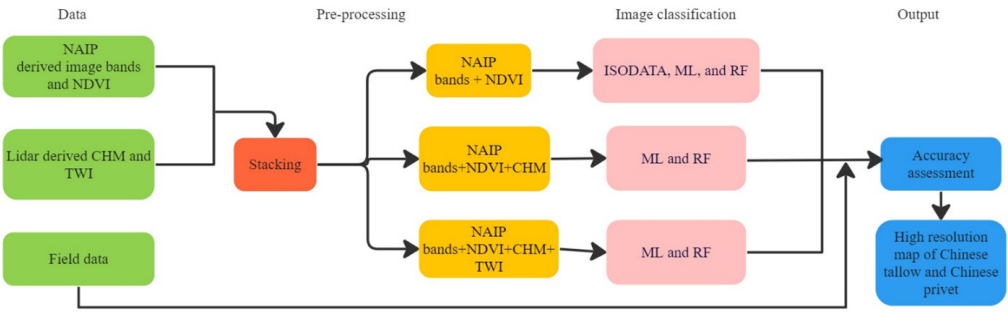

Figure 1 Workflow of the study.

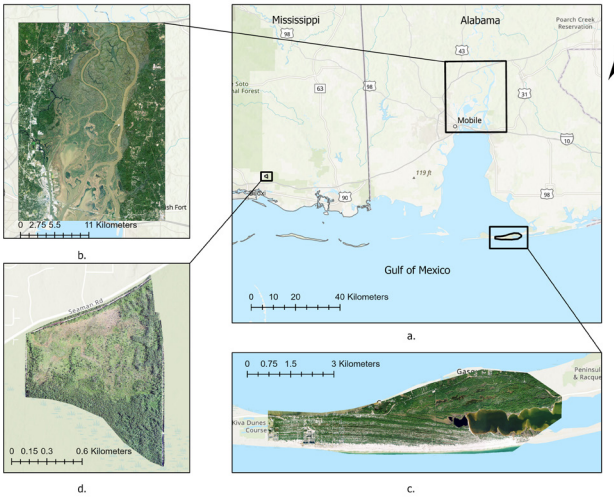

Figure 2 Map of the study area. a) Showing Alabama state and two study areas in the coastal region (Esri). b) Extent of Mobile Tensaw Wildlife Management Area (Survey 2019b). c) Extent of Bon Secour National Wildlife Refuge (Survey 2019b).

Data

Field data collection

Field data was collected in May 2021 along the road networks of Bon Secour and Mobile Tensaw. These study sites are located in coastal Alabama, thus only the road networks were accessible. On Mississippi Sandhill, the data collection was carried out in the western region of the wildlife refuge, where Tallow tree was dominant. Within Bon Secour and Mississippi Sandhill, only Tallow tree was observed and on Mobile Tensaw, both Tallow tree and Chinese privet were observed, based on a preliminary assessment of the study area. As a result, this study investigated the development of distribution maps of both Tallow tree and Chinese privet in Mobile Tensaw and examined only Tallow tree at Bon Secour and Mississippi Sandhill for species mapping. Location coordinates and percentage cover of the targeted invasive plants were recorded upon species sighting for all three study areas. This recorded actual presence and absence information of the invasives was used to validate the accuracy of maps.

Remote Sensing Data

Two sources of remotely sensed data were used, i.e., NAIP imagery and discrete return LiDAR data. The principal purpose of the NAIP is to make aerial imagery available within a year of acquisition. NAIP imagery acquired between the year 2019 and 2020 was collected in NAD83 UTM zone 16 N (unit: meter) from the USGS Earth Explorer (U.S. Geological Survey 2019). The image had a spatial resolution of 1 m and spectral resolution of four bands (RGB and Near Infrared).

Airborne LiDAR point clouds for the study area were acquired from USGS 3DEP. The primary goal of USGS 3DEP is to acquire nationwide LiDAR data and offer the first-ever national baseline of reliable high-resolution 3D point cloud data. Based on data availability, discrete return LiDAR data accessed from 2015 to 2020 was used for the study sites (Table 1). The LiDAR data was of Topographic Data Quality level 2 (QL2) with point density ranging from 2-3 points per m^2 (USGS 2020c) and point spacing ranging from 0.45-0.57 m (Table 1). LiDAR returns were classified into 7 land cover classes such as ground, urban, grassland, brushland, forested area, sawgrass, and mangrove/swamps (U.S. Geological Survey 2020b).

Data processing

NAIP imagery processing and derived products

Thirty, five and two NAIP Digital Ortho Quarter Quad tiles (DOQQs) were downloaded for Mobile Tensaw, Bon Secour, and Mississippi Sandhill, respectively. Those tiles were mosaicked and clipped to the extent of respective study area using ArcGIS Desktop (ESRI 2014). All four NAIP image bands (Blue, Green, Red and Near infrared) and NDVI were

used for image classification (Table 1). The original input bands were used since Kim et al. (2020) did not find an increase in classification accuracies using the normalized input bands. We decided not to convert the brightness values (or digital numbers) to reflectance values in order to calculate NDVI values following Kim et al. (2020). NDVI, a vegetation index with values ranging from -1 to +1 was computed from NAIP for image classification. Values closer to -1 represent unhealthy vegetation, +1 represent healthy vegetation, and 0 represent less or no vegetation. NDVI was calculated using brightness values of band 3 (Red) and band 4 (NIR) using the following formula:

$$NDVI = (BV_{NIR} - BVR_{ed}) / (BV_{NIR} + BVR_{ed})$$

where BVR_{ed} represents the brightness values (or digital numbers) of each pixel in the Red band (band 3) and BV_{NIR} represents the brightness values (or digital numbers) of each pixel in the Near Infrared band (band 4).

Table 1 Summary of data specification, acquisition date, and variables name for each study site.

Study site	Data	Acquisition date (Year)	LiDAR point spacing (m)	Variables name
Mobile	NAIP	2019		Red, Blue, Green and NIR band
Tensaw	LiDAR	2015 & 2019	0.49-0.55	CHM and TWI
Bon	NAIP	2019		449 (414/8/27)
Secour	LiDAR	2017	0.45	Red, Blue, Green and NIR band
Sandhill	NAIP	2020		CHM and TWI
Crane	LiDAR	2017	0.45	

LiDAR data processing and derived products

Some of the LiDAR data originally collected in Alabama State Plane West Zone (unit: feet) coordinate system was converted to NAD83 UTM zone 16 N (unit: meter) for consistency with NAIP imagery. The LiDAR point clouds were pre-processed to remove noise returns and derive heights above ground level using LAStools (Isenburg 2012) and ArcGIS. Points were filtered below 0 m and above 40 m. The height cut-off was defined based on the tallest tree recorded on the study site, i.e., 39.9 meters. After that, lasclip tool from LAStools was used to extract all returns of LiDAR data within the study area. One meter Canopy Height Models (CHMs) were derived from the height-normalized data for the study sites. To generate each CHM, a Digital Elevation Model (DEM), derived from ground returns of LiDAR was subtracted from Digital Surface Model (DSM), derived from first returns of LiDAR. In addition to that, Topographic Wetness Indices (TWI) for three study sites were also generated from respective LiDAR-derived DEM using ArcGIS.

Image classification

Training data

Five classes (water/coastal area, urban, other vegetation, Tallow tree, and Chinese privet) were defined for Mobile Tensaw. Four classes (water/coastal area, urban, other vegetation, and Tallow tree) were defined for Bon Secour and three classes (ground, other vegetation, and Tallow tree) were defined for Mississippi Sandhill, based on landcover of the respective study sites. Ten training samples were prepared for each class within each of the three study regions. A total of 120 training samples were prepared for the three study sites (Table 2). The training samples were selected based on the known locations of the classes using visual interpretation of the NAIP imagery. The samples for each class within the study sites were selected in such a way that they capture spectral variability and is a representative of the specific class. Jeffries-Matusita distance and Transformed Divergence measure, scaled between 0 and 2 (Sen et al. 2019), were used to determine the

Table 2 Summary of training samples used for ML and RF classification.

Study site	ML			RF		
	Train	Test*	Total	Train	Test*	Total
Mobile Tensaw	10*5	6*5	80	50	6*5	80
Bon Secour	10*4	6*4	64	40	6*4	64
Sandhill Crane	10*3	6*3	48	30	6*3	48
Total	120	72	192	120	72	192

spectral separability of the classes to ensure that the values were at least 1.9. Spectral separability greater than 1.9 indicated higher spectral separability of classes and is expected to enhance the classification accuracy. A separate test data, prepared based on ground truth were used for the validation of classification maps.

Image classifiers

The image classification was carried out using two datasets. First, using the NAIP stacked imagery alone and second, integrating the NAIP stacked imagery with LiDAR-derived CHM and TWI. For each study area, three image classification approaches i.e., unsupervised ISODATA clustering, supervised ML, and RF, a non-parametric machine learning algorithm were carried out using both datasets (Figure 1). Unsupervised classifiers group pixels based on similar spectral properties without the need for a prior knowledge. However, supervised classifiers use the representative sample pixels of specific classes provided by the training pixels to classify all other pixels in the image. The RF algorithm learns the relationship between predictor and response data (Horning 2010) and derives predictions from decision trees to provide reliable classification (Breiman 2001).

First image classification approach implemented was ISODATA clustering. ISODATA with only NAIP image was carried out as an exploratory step to determine spectrally separable classes. Based on the cluster of pixels that share similar spectral properties, a total of 15 color-coded classes were prepared with five iterations. After that, post classification was done to refine and reduce the number of classes using image interpretation. Each class was closely examined using classified and original imagery and the classes that share similar spectral property were combined to form five classified classes for Mobile Tensaw area. A similar process was applied to the other two study sites and four classified classes were obtained for Bon Secour and three classified classes were obtained for Mississippi Sandhill (Section Training data).

Second image classification approach was the ML classifier. It requires training data based on the known location of classes. The classifier assigns pixels to classes based on spectral properties of the training data. For Mobile Tensaw, fifty training samples for five classes were prepared (Table 2) using ENVI's Region of Interest (ROI) tool (Buller 2023). Similarly, for Bon Secour, forty training samples for four classes were prepared and for Mississippi Sandhill, thirty training samples for three classes were prepared for ML image classification. The non target classes such as water/coastal area, urban, ground, and other vegetation were merged into one class to properly discern the invasives in a classified map.

Third image classification approach was RF using ModelMap package in R Version 4.2.3 (R development Core Team 2010). ModelMap is an R package that allows for user-friendly modeling and mapping over vast geographic areas (Freeman et al. 2009). The categorical response variable and predictor variables were defined as demonstrated by (Freeman and Frescino 2018). A landcover classification map prepared using the ML classifier was used as a categorical response variable for each study area. Predictor variables used for RF were bands of NAIP imagery (red, green, blue, and near-infrared), a vegetation index derived from NAIP imagery (NDVI), and LiDAR-derived variables (CHM and TWI). The user defined variables are used to select the splits at each node (mtry) on a decision tree. Based on majority voting of number of trees (ntrees) the final class is selected. The major benefit of employing RF is its ability to rank the importance of each input variable added in the model. The higher the rank of a variable, the more it contributes to image classification.

Accuracy assessment

The classification accuracy of NAIP stacked and NAIP-LiDAR stacked image were assessed using confusion matrices in the ENVI

software. The separate test dataset, created using presence and absence information from ground truth, was used to assess the accuracy of each classification approach used for the study. The overall classification accuracy was estimated by calculating the proportion of correctly classified pixels of the land cover classes out of the total pixels in the classified image. Along with the overall classification accuracy, the Kappa coefficient (k), an agreement between known and predicted value, was also estimated. Producer's Accuracy (PA) and User's Accuracy (UA) for each of the land cover classes were also reported. PA is a measure of the precision with which each class is produced by an analyst on a classification map, whereas UA measures how accurate each class is from a map user's point of view. The results of accuracy assessment were mainly focused on the targeted invasive plants i.e., Tallow tree and Chinese privet.

Results

Three image classification approaches (ISODATA, ML, and RF) were implemented on two input data sources for three coastal sites of Alabama and Mississippi. NAIP stacked image was used for ISODATA classification, whereas input datasets, such as NAIP stacked image and NAIP stacked with LiDAR-derived variables were used for ML and RF. Results were summarized based on the study sites, image classification algorithms and datasets. Figures represent the distribution of Tallow tree and Chinese privet produced with maximum OA and k for different study sites. Tables represent the summary of classification results including OA, k, PA, UA and confusion matrices for all three study sites (Table 3 – Table 6).

Table 3 Summary of results obtained from the accuracy assessment.

Study site	Method	Datasets		
		NAIP	NAIP+CHM	NAIP+CHM+TWI
Mobile Tensaw River Delta	ISODATA	OA=54.42%, k=0.43		
		PA=77.10%, UA=59.78%		
		PA*=29.72%, UA*=100%		
	ML	OA=76.86%, k=0.71	OA=77.42%, k=0.71	OA=85.63%, k=0.82
		PA=97.14%, UA=70.83%	PA=67.62%, UA=69.61%	PA=91.43%, UA=98.97%
		PA*=79.82, UA*=75.65%	PA*=89.91, UA*=100%	PA*=89.91%,UA*=89.09%
	RF	**OA=87.5%, k=0.84**	OA=82.64%, k=0.78	OA=80.03%, k=0.75
		PA=96.19%, UA=84.17%	PA=99.05%, 84.55%	PA=99.05%, UA=85.95%
		PA*=94.50%, UA*=89.57%	PA*=94.50%, UA*=93.6%	PA*=97.25%,UA*=92.17%
Bon Secour National Wildlife Refuge	ISODATA	OA=83.90%, k=0.78		
		PA=54.95%, UA=100%		
	ML	OA=80.93%, k=0.74	OA=93.64%, k=0.91	**OA=95.33%, k=0.93**
		PA=71.93%, UA=100%	PA=82.46%, UA=100%	PA=96.49%, UA=100%
	RF	OA=89.40%, k=0.85	OA=94.29%, k=0.88	OA=90.25%, k=0.86
		PA=100%, UA=78%	PA=98.26%, UA=99.12%	PA=100%, UA=80.28%
Mississippi Sandhill Crane National Wildlife Refuge	ISODATA	OA= 89.13%, k=0.83		
		PA=69.57%, UA=100%		
	ML	OA= 87.28%, k=0.81	OA=90.67%, k=0.85	**OA=93.22%, k=0.89**
		PA=87.18%, UA=89.47%	PA=94.87%, UA=100%	PA=94.87%, UA=97.37%
	RF	OA=88.98%, k=0.83	OA=90.67%, k=0.85	OA=92.37%, k=0.88
		PA=89.74%, UA=100%	PA=94.87%, UA=100%	PA=97.44%, UA=100%

Note:PA=Producer's Accuracy of Tallow tree, UA=User's Accuracy of Tallow tree, PA*=Producer's Accuracy of Chinese privet, UA*=User's Accuracy of Chinese privet. The highlighted OAs and k are the highest for the study site and are further explained in Table 4 - Table 6.

Table 4 Confusion matrix prepared by comparing classified image generated from RF on NAIP stacked image against ground truths of Mobile Tensaw area.

Random Forest classified image	Ground Truth (Pixels)					
Class	Water	Urban	Other vegetation	Tallow	Privet	Total
Water	**81**	3	0	0	1	85
Urban	3	**103**	0	0	0	106
Other vegetation	21	0	**81**	4	4	110
Tallow	0	0	18	**101**	1	120
Privet	0	0	12	0	**103**	115
Total	105	106	111	105	109	**536**

Note: Total number of correctly classified pixels = (81+103+81+101+103) = 469. Overall classification accuracy = 469/536 =87.50%. Kappa coefficient = 0.84

Table 5 Confusion matrix prepared by comparing classified image generated from ML on NAIP-LiDAR stacked image against ground truths of Bon Secour area.

Maximum Likelihood classified image	Ground Truth (Pixels)				
Class	Water	Urban	Other vegetation	Tallow	Total
Water	**56**	0	9	0	65
Urban	0	**80**	0	0	80
Other vegetation	0	0	**34**	2	36
Tallow	0	0	0	**55**	55
Total	56	80	43	57	**236**

Note: Total number of correctly classified pixels = (56+80+34+55) = 225. Overall classification accuracy = 225/236 = 95.33%. Kappa coefficient = 0.93.

Table 6 Confusion matrix prepared by comparing classified image generated from ML on NAIP-LiDAR stacked image against ground truths of Mississippi Sandhill area.

Maximum Likelihood classified image	Ground Truth (Pixels)			
Class	Ground	Other vegetation	Tallow	Total
Ground	**41**	5	0	46
Other vegetation	0	**32**	2	34
Tallow	0	1	**37**	38
Total	41	38	39	**118**

Note: Total number of correctly classified pixels = (41+32+37) = 110. Overall classification accuracy = 110/118 = 93.22%. Kappa coefficient = 0.89.

Confusion matrices using ground truth ROIs were used to conduct accuracy assessment. The matrix contains information of each image classification including the correctly classified pixels and mis-classified pixels. In general, grassland, shrubs, and algal concentration were confused with Tallow tree and Chinese privet (Table 4 - Table 6).

Mobile Tensaw River Delta

The OA (54.42%) and k (0.43) of the classification map using ISODATA increased to 76.86% and 0.71 respectively using ML on NAIP stacked imagery (Table 3). The OA further increased from 76.86% to 77.42% using NAIP and CHM stacked imagery. Additionally, the OA (85.63%) and k (0.82) was obtained with NAIP stacked with LiDAR-derived CHM and TWI using ML. With the same dataset and classification algorithm, we observed increased PA (89.91%) and UA (89.09%) for Chinese privet. The UA for Chinese privet increased from 75.65% to 89.09% on adding LiDAR-derived CHM and TWI to NAIP stacked imagery. Similarly, the UA of Tallow tree also increased from 70.83% to 98.97 with the same approach.

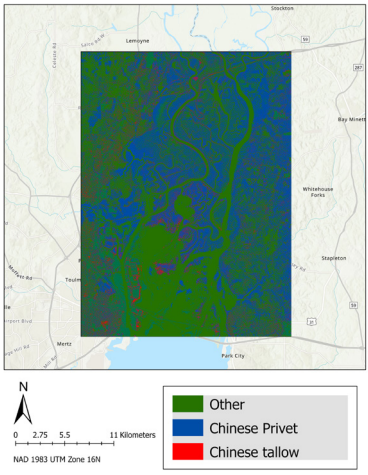

Figure 3 Classified image of Mobile Tensaw Wildlife Management Area showing the distribution of Tallow tree and Chinese privet using RF on NAIP stacked imagery with the highest OA and k. The green area represents other (water, urban, and other vegetation), red area represents Tallow tree, and blue area represents Chinese privet.

Among all classification algorithms and datasets used, the highest OA (87.5%) and the highest k (0.84) was obtained with RF using NAIP stacked imagery (Figure 3). The addition of LiDAR-derived CHM and TWI did not contribute to increase the OA and k as compared to NAIP stacked image using RF. However, the PA and UA of Tallow tree increased from 96.19% and 84.17% to 99.05% and 85.95% respectively, on adding LiDAR-derived CHM and TWI to NAIP stacked imagery using RF. Likewise, the PA and UA of Chinese privet increased from 94.50% and 89.57% to 97.25% and 92.17% respectively with the same dataset and method (Table 3).

Bon Secour National Wildlife Refuge

The OA (83.90%) and k (0.78) of the classification map using ISODATA increased to 80.93% and 0.74 respectively, using ML on NAIP stacked image (Table 3). The OA further increased from 80.93% to 93.64% using NAIP and CHM stacked image. Moreover, the highest OA (95.33%) and k (0.93) was obtained with NAIP stacked with LiDAR-derived CHM and TWI using ML (Figure 4). The same dataset and method that produced highest OA and k gave the highest PA (96.49%) and UA (100%) for classifying Tallow tree. Besides that, we observed an increase in PAs for classifying Tallow tree with the addition of LiDAR-derived variables as compared to NAIP stacked image alone using ML. Similarly, with RF classification the OA and k increased from 89.4% and 0.85 to 94.29% and 0.88 respectively, on adding LiDAR-derived CHM to NAIP stacked image. However, the accuracies did not increase further on adding TWI to the dataset with RF classification.

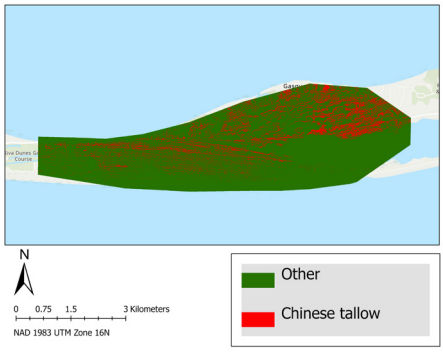

Figure 4 Classified image of Bon Secour National Wildlife Reserve showing the distribution of Tallow tree using ML for NAIP stacked with LiDAR-derived CHM and TWI. The green area represents other (water, urban, and other vegetation) and red area represents the distribution of Tallow tree. This map has the highest OA, k, PA, and UA for classifying Tallow tree among the classification approaches used.

Mississippi Sandhill Crane National Wildlife Refuge

We obtained OA (89.13%) and k (0.83) for the classification map using ISODATA. The classification accuracy increased from 87.28% to 90.67% on adding LiDAR-derived CHM to NAIP stacked image using ML. The highest OA (93.22%) and k (0.89) was obtained with NAIP stacked image and LiDAR derived CHM and TWI using ML (Figure 5). The PA and UA

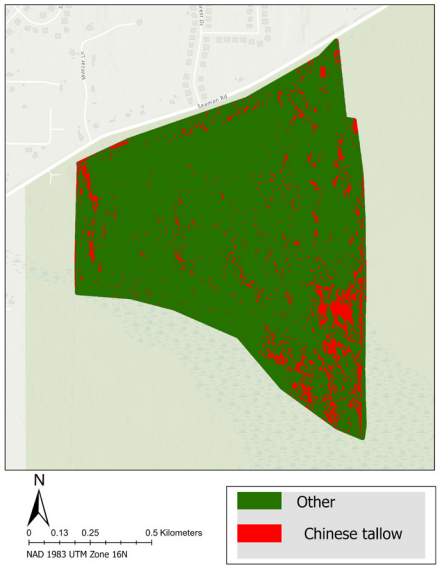

Figure 5 Classified image of Mississippi Sandhill Crane National Wildlife refuge (one unit amongst the 99 units representing western Wildlife Refuge area) showing the distribution of Tallow tree using ML for NAIP stacked with LiDAR-derived CHM and TWI. The green area represents other (ground and other vegetation) and red area represents the distribution of Tallow tree. This maps the highest OA and k among the classification approaches used.

for classifying Tallow tree increased on adding LiDAR derived CHM and TWI to NAIP stacked image as compared to NAIP stacked image alone. Likewise, with RF classification the OA and k increased from 88.98% and 0.83 to 90.67% and 0.85 respectively, on adding LiDAR-derived CHM to NAIP stacked image. The OA further increased to 92.37% with LiDAR derived TWI added to the CHM and NAIP stacked image (Table 3).

Discussion

The study investigated techniques for mapping the distribution of Tallow tree and Chinese privet within ecologically sensitive coastal areas, with focus on the coastal region of Alabama and Mississippi in the southeastern United States. A combination of bands and NDVI derived from NAIP imagery and LiDAR-derived CHM and TWI were examined for each classification approach used. Evidently, the OA, PA, UA, and k obtained from different classification approaches varied over the study area.

Among all classification approaches carried out on Mobile Tensaw area, RF on NAIP stacked image outperformed ISODATA and ML. Jensen et al. (2020) and Shoot et al. (2021) support machine learning algorithm (e.g., RF) as a robust classifier for natural resource data. Shoot et al. (2021) achieved the highest OA (78%) and k (0.66) with RF classification algorithm using vegetation indices and LiDAR-derived canopy height metrics. The variables importance showed that near infrared band followed by NDVI were the most important band with NAIP stacked image as the input data source. With the added CHM and TWI to NAIP stacked image, the most important variables were NDVI followed by near infrared band and TWI. Kim et al. (2020) found near infrared and DEM as the most important variables among their classifications. On Bon Secour and Mississippi Sandhill area, ML classifier produced better OA and k as compared to ISODATA and RF. In general, ML classifier performed well over the smaller study sites (Bon Secour and Mississippi Sandhill) as compared to the larger study site (Mobile Tensaw). Paola and Schowengerdt (1995) noted that the ML classifier is sensitive to spectral properties of classes and performs better for small areas with homogeneous forest stands. The separation of classes in such cases is more straightforward and there is less confusion between classes yielding higher accuracy.

Regardless of the algorithms used for all three study sites, we observed an increased overall classification accuracy with added LiDAR-derived variables, such as CHM and TWI to the NAIP stacked image, as compared to the NAIP stacked image alone. In coastal regions, elevation and water govern the dynamics of vegetation that grow there. Based on the field observation of our target invasives i.e., Tallow tree and Chinese privet grow mostly on low elevation area with abundant water. Hence, it was difficult to achieve spectral separability of training samples between classes with NAIP stacked image only. We observed an increased OA and PA for classifying Tallow tree and Chinese privet after adding the CHM and TWI to NAIP stacked image. The addition of these LiDAR-derived variables enhanced the capability to discern Tallow tree and Chinese privet with added vegetation structure and moisture information. Evaluation of accuracy assessment also shows that the other vegetation class including grassland and shrubland in prairie ecosystem and algal concentration in water were separable from Tallow tree and Chinese privet (Table 4). Studies have demonstrated the benefits of combining structural (LiDAR) and spectral (imagery) data in this regard. For example, Große-Stoltenberg et al. (2016) and Hantson et al. (2012) conveyed higher classification accuracies with the aerial imagery combined with LiDAR than the aerial imagery alone.

Most of the coastal regions of southern Alabama and Mississippi are not accessible

due to the floodplains. This highlights the use of remote sensing techniques for potential mapping of invasives, especially on the inaccessible study sites. Invasive plants can be detected remotely, given distinct morphology and seasonality. Cavender-Bares et al. (2020) showed that when the target invasives have unique phenology, it is easier to distinguish invasives from the native species. For instance, Ramsey et al. (2002) showed that the leaves of Tallow tree turn red during the fall season, when it is senescing, making it distinct from other native species. However, not all Tallow trees senesce at the same rate, there are chances of confusion with other plant species turning red, and acquiring data of desired season can be costly. For this study, we developed a framework with a cost-effective approach using freely available data (NAIP imagery and airborne LiDAR) and attained good accuracies to detect Tallow tree and Chinese privet. We produced high resolution (1 m) distribution maps of Tallow tree and Chinese privet within the southern coastal USA.

We recommended using the remotely sensed data of senescing season, if available, for the tallow dominant area to attain better accuracy. We also suggest the use of drone survey for collecting presence and absence data of invasive species from the inaccessible areas for better accuracy.

Joshi et al. (2004) conveyed that remote sensing has been most applied for mapping canopy-dominant species so far. Remote sensing techniques used for detecting invasives plants have mainly dealt with overstory invasives (Ramsey et al. 2002, Randall 2015, Große-Stoltenberg et al. 2016). But all invasives do not dominate the canopy. Many invasive plants of concern are understory, where the application of remote sensing technique is tricky for species detection. Due to the difficulty of mapping understory invasives, these invaders have received little attention. Chinese privet is an understory shrub, concealed by the canopy of Tallow tree and other overstory vegetation, that makes it challenging to detect. A study conducted by Cash et al. (2020) leveraged the potential to map Chinese privet over a small area of 23 km^2 using freely available satellite image from Landsat 8 and Sentinel 2. Another study by Singh et al. (2015) used data intensive methodology of mapping Chinese privet using airborne LiDAR and IKONOS imagery. In our study, the capability of mapping Chinese privet using LiDAR-derived variables integrated with NAIP imagery was demonstrated and thus, recommended as a feasible approach for developing distribution map of invasives in inaccessible sites. We suggest exploring the combination of input data sources derived from LiDAR such as canopy cover model, canopy density model, textures (data range, contrast, entropy), and topographic roughness. We further recommend post processing approaches with different window sizes to produce accurate vegetation maps.

Conclusions

The study examined different mapping approaches by using free and publicly available remote sensing data for invasive species mapping. In Mobile Tensaw, RF algorithm achieved the highest OA of 87.5% using NAIP stacked imagery. In Bon Secour, the ML classifier achieved the highest OA of 95.33% using the CHM and TWI integrated with NAIP imagery. Similarly, the same classifier and input dataset produced the highest OA of 93.22% in Mississippi Sandhill. Regardless of the study sites and algorithms used, adding LiDAR-derived variables to NAIP stacked image increased the classification accuracies of Tallow tree and Chinese privet. The RF algorithm outperformed ISODATA and ML classifier while classifying Tallow tree and Chinese privet in Mobile Tensaw. With the same algorithm, the highest classification accuracies were achieved for Tallow tree in Mississippi Sandhill, whereas in Bon Secour, the highest classification accuracies for Tallow tree were achieved with the ML classifier. The workflow

used by this study offers an inexpensive, reliable, and high-resolution data framework alternative to purchasing commercial data. The study provides a spatially explicit baseline inventory map of vital invasive species of the region that contributes to developing a framework for broader-scale mapping.

Acknowledgements

We would like to thank the Alabama Agricultural Experiment Station and Hatch program of the National Institute of Food and Agriculture, United States Department of Agriculture for funding the project. We would also like to extend our gratitude to the geospatial analytics lab of the College of Forestry, Wildlife, and Environment, Auburn University.

References

Albdel-Rahman E.M., Mutanga O., Adam E., & Ismail R. 2014. Detecting Sirex noctilio grey-attacked and lightning-struck pine trees using airborne hyperspectral data, random forest and support vector machines classifiers. ISPRS Journal of Photogrammetry and Remote Sensing, 88: 48-59. https://doi.org/10.1016/j.isprsjprs.2013.11.013

ALIPC 2019. Alabama Invasive Plant Council. https://www.se-eppc.org/alabama/

Asner G.P., Knapp D.E., Kennedy-Bowdoin T., Jones M.O., Martin R.E., Boardman J., & Hughes R.F. 2008. Invasive species detection in Hawaiian rainforests using airborne imaging spectroscopy and LiDAR. Remote Sensing of Environment, 112: 1942-1955. https://doi.org/10.1016/j.rse.2007.11.016

Barnett J.M. 2016. The impact of Chinese privet (*Ligustrum sinense*) on the survival and re-establishment of native plants at the dallas floodway extension. Masters thesis, Department of Geography, University of North Texas, Denton, 75 p.

Benez-Secanho F.J., Grebner D.L., Ezell A.W., & Grala R.K. 2018. Financial trade-offs associated with controlling Chinese privet (*Ligustrum sinense* Lour.) in forestlands in the southern USA. Journal of Forestry, 116: 236-244. https://doi.org/10.1093/jofore/fvy003

Bork E.W., & Su J.G. 2007. Integrating LIDAR data and multispectral imagery for enhanced classification of rangeland vegetation: A meta analysis. Remote Sensing of Environment, 111: 11-24. https://doi.org/10.1016/j.rse.2007.03.011

Bradley B.A. 2014. Remote detection of invasive plants: a review of spectral, textural and phenological approaches. Biological Invasions, 16: 1411-1425. https://doi.org/10.1007/s10530-013-0578-9

Breiman L. 2001. Random forests. Machine Learning, 45: 5-32. https://doi.org/10.1023/A:1010933404324

Buller I.D. 2023. The Environment for Visualising Images (ENVI). L3Harris Geospatial Solutions. https://cran.r-project.org/package=envi

Bush B.M., Ulyshen M.D., & Batzer D.P. 2020. Effects of Chinese privet (*Ligustrum sinense*) invasion on decomposition and litter-dwelling invertebrates in Southeastern US floodplain forests. Biological Invasions, 22, 1957-1965. https://doi.org/10.1007/s10530-020-02228-2

Calvino-Cancela M., Mendez-Rial R., Reguera-Salgado J., & Martin-Herrero J. 2014. Alien plant monitoring with ultralight airborne imaging spectroscopy. PloS one, 9: e102381. https://doi.org/10.1371/journal.pone.0112031

Cash J.S., Anderson C.J., & Marzen L. 2020. Evaluating free and simple remote sensing methods for mapping Chinese privet (Ligustrum sinense) invasions in hardwood forests. SN Applied Sciences, 2: 1-11. https://doi.org/10.1007/s42452-020-2596-4

Cavender-Bares J., Gamon J.A., & Townsend P.A. 2020. Remote sensing of plant biodiversity. Springer Nature.

Chan J.C.-W., Beckers P., Spanhove T., & Borre J.V. 2012. An evaluation of ensemble classifiers for mapping Natura 2000 heathland in Belgium using spaceborne angular hyperspectral (CHRIS/Proba) imagery. International Journal of Applied Earth Observation and Geoinformation, 18: 13-22. https://doi.org/10.1016/j.jag.2012.01.002

Dubayah R.O., & Drake J.B. 2000. Lidar remote sensing for forestry. Journal of Forestry, 98: 44-46. https://doi.org/10.1093/jof/98.6.44

Ehrenfeld J.G. 2010. Ecosystem consequences of biological invasions. Annual Review of Ecology, Evolution, and Systematics, 41: 59-80. https://doi.org/10.1146/annurev-ecolsys-102209-144650

ESRI 2014. Arc GIS Desktop. Environmental Systems Research Institute. http://resources.arcgis.com/en/help/main/10.2/index.html

Fantle-Lepczyk J.E., Haubrock P.J., Kramer A.M., Cuthbert R.N., Turbelin A.J., Crystal-Ornelas R., Diagne C., & Courchamp F. 2022. Economic costs of biological invasions in the United States. Science of the Total Environment, 806, 151318. https://doi.org/10.1016/j.scitotenv.2021.151318

Foard M. 2014. Causes and consequences of Chinese privet

(*Ligustrum sinense* Lour.) invasion in hydrologically altered forested wetlands. Arkansas State University.

Freeman E., Frescino T., & Moisen G. 2009. ModelMap: an R Package for model creation and map production using Random Forest and Stochastic Gradient Boosting. CRAN package.

Freeman E., & Frescino T. 2018. Modeling and map production using random forest and related stochastic models.

Gislason P.O., Benediktsson J.A., & Sveinsson J.R. 2006. Random forests for land cover classification. Pattern Recognition Letters, 27: 294-300. https://doi.org/10.1016/j.patrec.2005.08.011

Große-Stoltenberg A., Hellmann C., Werner C., Oldeland J., & Thiele J. 2016. Evaluation of continuous VNIR-SWIR spectra versus narrowband hyperspectral indices to discriminate the invasive *Acacia longifolia* within a Mediterranean dune ecosystem. Remote Sensing, 8: 334. https://doi.org/10.3390/rs8040334

Ham J., Chen Y., Crawford M.M., & Ghosh J. 2005. Investigation of the random forest framework for classification of hyperspectral data. IEEE Transactions on Geoscience and Remote Sensing, 43: 492-501. https://doi.org/10.1109/TGRS.2004.842481

Handley L.R., Spear K.A., Jones S., & Thatcher C.A. 2013. Mobile Bay. https://pubs.er.usgs.gov/publication/70041785

Hantson W., Kooistra L., & Slim P.A. 2012. Mapping invasive woody species in coastal dunes in the N etherlands: a remote sensing approach using LIDAR and high-resolution aerial photographs. Applied Vegetation Science, 15: 536-547. https://doi.org/10.1111/j.1654-109X.2012.01194.x

Hanula J.L., & Horn S. 2009. Impact of Chinese privet and its removal on pollinator diversity and abundance. In, 20th US Department of Agriculture Interagency Research Forum on Invasive Species 2009, Citeseer, 74 p.

Hart J.L., & Holmes B.N. 2013. Relationships between *Ligustrum sinense* invasion, biodiversity, and development in a mixed bottomland forest. Invasive Plant Science and Management, 6: 175-186. https://doi.org/10.1614/IPSM-D-12-00050.1

Hawthorne T., Elmore V., Strong A., Bennett-Martin P., Finnie J., Parkman J., Harris T., Singh J., Edwards L., & Reed J. 2015. Mapping non-native invasive species and accessibility in an urban forest: A case study of participatory mapping and citizen science in Atlanta, Georgia. Applied Geography, 56: 187-198. https://doi.org/10.1016/j.apgeog.2014.10.005

Heckbert S., Costanza R., Poloczanska E., & Richardson A. 2011. 12.10 – Climate regulation as a service from estuarine and coastal ecosystems. Treatise on Estuarine and Coastal Science: 199-216. https://doi.org/10.1016/B978-0-12-374711-2.01211-0

Horning N. 2010. Random Forests: An algorithm for image classification and generation of continuous fields data sets.

Huang C.-y., & Asner G.P. 2009. Applications of remote sensing to alien invasive plant studies. Sensors, 9: 4869-4889. https://doi.org/10.3390/s90604869

Isenburg M. 2012. LAStools-efficient tools for LiDAR processing. rapidlasso. http://www.cs.unc.edu/~isenburg/lastools

Ismail R., Mutanga O., & Peerbhay K. 2016. The identification and remote detection of alien invasive plants in commercial forests: An Overview. South African Journal of Geomatics, 5: 49-67. https://doi.org/10.4314/sajg.v5i1.4

Jensen T., Seerup Hass F., Seam Akbar M., Holm Petersen P., & Jokar Arsanjani J. 2020. Employing machine learning for detection of invasive species using sentinel-2 and aviris data: The case of Kudzu in the United States. Sustainability, 12: 3544. https://doi.org/10.3390/su12093544

Joshi C., De Leeuw J., & Van Duren I.C. 2004. Remote sensing and GIS applications for mapping and spatial modelling of invasive species. In Proceedings of ISPRS, B7 p. http://www.itc.nl/library/Papers_2004/peer_conf/joshi.pdf

Kim J., Popescu S.C., Lopez R.R., Wu X.B., & Silvy N.J. 2020. Vegetation mapping of No Name Key, Florida using lidar and multispectral remote sensing. International Journal of Remote Sensing, 41: 9469-9506. https://doi.org/10.1080/01431161.2020.1800125

Klepac J., Rummer R.B., Hanula J.L., & Horn S. 2007. Mechanical removal of Chinese privet. Res. Pap. SRS-43. Asheville, NC: US Department of Agriculture, Forest Service, Southern Research Station. 5 p., 43. https://doi.org/10.2737/SRS-RP-43

Liang W., Abidi M., Carrasco L., McNelis J., Tran L., Li Y., & Grant J. 2020. Mapping vegetation at species level with high-resolution multispectral and lidar data over a large spatial area: a case study with Kudzu. Remote Sensing, 12: 609. https://doi.org/10.3390/rs12040609

Loewenstein N.J., & Loewenstein E. 2005. Non-native plants in the understory of riparian forests across a land use gradient in the Southeast. Urban Ecosystems, 8: 79-91. https://doi.org/10.1007/s11252-005-1420-7

Matongera T.N., Mutanga O., Dube T., & Lottering R.T. 2018. Detection and mapping of bracken fern weeds using multispectral remotely sensed data: a review of progress and challenges. Geocarto International, 33: 209-224. https://doi.org/10.1080/10106049.2016.1240719

Michez A., Piégay H., Jonathan L., Claessens H., & Lejeune P. 2016. Mapping of riparian invasive species with supervised classification of Unmanned Aerial System (UAS) imagery. International Journal of Applied Earth Observation and Geoinformation, 44: 88-94. https://doi.org/10.1016/j.jag.2015.06.014

Mohler R.L., & Morse J.M. 2022. Using UAV imagery to map invasive *Phragmites australis* on the Crow Island State Game Area, Michigan, USA. Wetlands Ecology and Management, 30: 1213-1229. https://doi.org/10.1007/s11273-022-09890-4

Montez R.D., Saenz D., Martynova-Van Kley A., Van Kley J., Nalian A., & Farrish K. 2021. The influence of Chinese tallow (*Triadica sebifera*) leaf litter on water quality and microbial community composition. Aquatic Ecology, 55: 265-282. https://doi.org/10.1007/s10452-020-09828-z

Ng B., Quinete N., Maldonado S., Lugo K., Purrinos J., Briceño H., & Gardinali P. 2021. Understanding the occurrence and distribution of emerging pollutants and endocrine disruptors in sensitive coastal South Florida Ecosystems. Science of the Total Environment, 757: 143720. https://doi.org/10.1016/j.scitotenv.2020.143720

Order Executive 1999. 13112. 1999. Invasive species. Federal Register, 64: 6183-6186.

Paola J.D., & Schowengerdt R.A. 1995. A review and analysis of backpropagation neural networks for classification of remotely-sensed multi-spectral imagery. International Journal of Remote Sensing, 16: 3033-3058. https://doi.org/10.1080/01431169508954607

Popescu S.C. 2007. Estimating biomass of individual pine trees using airborne lidar. *Biomass and Bioenergy, 31*, 646-655. https://doi.org/10.1016/j.biombioe.2007.06.022

R development Core Team 2010. R: A language and environment for statistical computing In: R Foundation for Statistical Computing. http://www.R-project.org

Ramsey E.W., Nelson G.A., Sapkota S.K., Seeger E.B., & Martella K.D. 2002. Mapping Chinese tallow with color-infrared photography. Photogrammetric Engineering & Remote Sensing, 68: 251-255.

Randall J.P. 2015. Remote-sensing detection of invasive Chinese tallow (*Triadica sebifera*) in a Floodplain Environment. Texas A&M University.

Sen R., Goswami S., & Chakraborty B. 2019. Jeffries-Matusita distance as a tool for feature selection. In, 2019 International Conference on Data Science and Engineering (ICDSE), IEE, 15-20. https://doi.org/10.1109/ICDSE47409.2019.8971800

Shoot C., Andersen H.-E., Moskal L.M., Babcock C., Cook B.D., & Morton D.C. 2021. Classifying forest type in the national forest inventory context with airborne hyperspectral and lidar data. Remote Sensing, 13: 1863. https://doi.org/10.3390/rs13101863

Singh K.K., Davis A.J., & Meentemeyer R.K. 2015. Detecting understory plant invasion in urban forests using LiDAR. International Journal of Applied Earth Observation and Geoinformation, 38: 267-279. https://doi.org/10.1016/j.jag.2015.01.012

U.S. Fish and Wildlife Service 2023a. Bon Secour National Wildlife Refuge. https://www.fws.gov/refuge/bon-secour

U.S. Fish and Wildlife Service 2023b. Mississippi Sandhill Crane National Wildlife Refuge. https://www.fws.gov/refuge/mississippi-sandhill-crane

U.S. Geological Survey 2019. Earth Explorer. https://earthexplorer.usgs.gov/

U.S. Geological Survey 2020a. 3D Elevation Program Lidar Point Cloud. https://apps.nationalmap.gov/downloader/

U.S. Geological Survey. 2020c. Topographic Data Quality Levels (QLs). https://www.usgs.gov/3d-elevation-program/topographic-data-quality-levels-qls

Ustin S.L., DiPietro D., Olmstead K., Underwood E., & Scheer G.J. 2002. Hyperspectral remote sensing for invasive species detection and mapping. IEEE International Geoscience and Remote Sensing Symposium, IEEE, pp. 1658-1660. https://doi.org/10.1109/IGARSS.2002.1026212

Wang H.-H. 2011. Occupation, dispersal, and economic impact of major invasive plant species in southern US forests. Doctor of Philosophy dissertation, Forestry, Texas A&M University, College Station, 181 p.

Wilcove D.S., Rothstein D., Dubow J., Phillips A., & Losos E. 1998. Quantifying threats to imperiled species in the United States. BioScience, 48: 607-615. https://doi.org/10.2307/1313420

Wilcox J., & Beck C.W. 2007. Effects of *Ligustrum sinense* Lour. (Chinese privet) on abundance and diversity of songbirds and native plants in a southeastern nature preserve. Southeastern Naturalist, 6: 535-550. https://www.jstor.org/stable/4541047

Yang S., Fan Z., Liu X., & Ezell A.W. 2021. Predicting the spread of Chinese tallow (*Triadica sebifera*) in the southeastern United States forestland: Mechanism and risk factors at the regional scale. Forest Ecology and Management, 482: 118892. https://doi.org/10.1016/j.foreco.2020.118892

Zedler, J.B., & Kercher, S. (2004). Causes and consequences of invasive plants in wetlands: opportunities, opportunists, and outcomes. Critical Reviews in Plant Sciences, 23: 431-452. https://doi.org/10.1080/07352680490514673

Zuberi M.I., Gosaye T., & Hossain S. 2014. Potential threat of alien invasive species: *Parthenium hysterophorus* L. to subsistence agriculture in Ethiopia. Sarhad Journal of Agriculture, 30: 117-125.